Numerical Simulations of Cohesive Sediment Transportation in Coastal Waters Considering Time-dependent Sediment Resuspension and Deposition

Hiramatsu, Kazuaki
Laboratory of Drainage and Water Environment, Division of Regional Environment Science, Department of Bioproduction Environmental Science, Faculty of Agriculture, Kyushu University

Shikasho, Shiomi
Laboratory of Drainage and Water Environment, Division of Regional Environment Science, Department of Bioproduction Environmental Science, Faculty of Agriculture, Kyushu University

Mori, Ken
Laboratory of Bioproduction and Environment Information Science, Division of Bioproduction and Environment Information Science, Department of Bioproduction Environmental Science, Faculty of Agriculture, Kyushu University

https://doi.org/10.5109/24416

出版情報：九州大学大学院農学研究院紀要. 46 (1), pp.1-14, 2001-10-30. Kyushu University
バージョン：
権利関係：

J. Fac. Agr., Kyushu Univ., **46** (1), 1–14 (2001)

Numerical Simulations of Cohesive Sediment Transportation in Coastal Waters Considering Time-dependent Sediment Resuspension and Deposition

Kazuaki HIRAMATSU, Shiomi SHIKASHO and Ken MORI***

Laboratory of Drainage and Water Environment, Division of Regional Environment Science, Department of Bioproduction Environmental Science, Faculty of Agriculture, Kyushu University, Fukuoka 812–8581, Japan

(Received June 22, 2001 and accepted July 11, 2001)

The Ariake Sea, which is a typical semi-closed bay located in Kyushu Island, western Japan, has a maximum tidal range of about 6 m in spring tide and has vast tidal flats composed of both sandy bottom areas and muddy bottom areas. In this study, 2-dimensional depth-averaged finite difference numerical models have been developed for predicting the tidal flow velocity and suspended sediment concentration in the Ariake Sea. In the suspended sediment transportation model, time-dependent sediment resuspension and deposition were modeled as response to the tidal flow by considering the presence of cohesive bottom sediment. The model results were compared with the in situ measurements of suspended sediment concentration and tidal flow velocity at several stations in Isahaya Bay located at the western part of the Ariake Sea, and with the concentration map of suspended sediment concentration estimated from the Landsat Thematic Mapper image. The results indicated that the models were able to accurately reproduce the measured values of suspended sediment concentration and tidal flow velocity and the estimated general pattern of the concentration map.

INTRODUCTION

Estuaries serve as spawning and nursery grounds for many important species of fish and shellfish as well as being conduits through which nutrients pass into productive coastal waters. Suspended sediment is a major problem in aquatic ecosystems of estuaries and coastal waters around the world. Suspended sediment affects water quality, primary productivity, fish production and the aesthetic value of coastal areas. For this reason, the prediction of tidal flow and suspended sediment transportation in coastal waters is one of the most important tasks in coastal engineering and related areas. The prediction is very difficult, however, not only because the sediment resuspension and deposition phenomena are very complex but also because the sediment distribution on the seabed is non-homogeneous.

The purpose of this study is to establish models to simulate the suspended sediment transportation in estuaries and coastal waters, especially in the Ariake Sea. The location and seabed topography of the Ariake Sea are shown in Fig. 1, in which the land area is indicated to be TP +5 m (TP 0 m approximately corresponds to the mean sea level). The Ariake Sea is a typical semi-closed bay located in Kyushu Island, western Japan. In

* Laboratory of Bioproduction and Environment Information Sciences, Division of Bioproduction and Environment Information Sciences, Department of Bioproduction Environmental Science, Faculty of Agriculture, Kyushu University, Fukuoka 812–8581, Japan

** Corresponding author (E-mail: hiramatu@agr.kyushu-u.ac.jp)

spring tide, the Ariake Sea has a maximum tidal range of about 6 m and has vast tidal flats composed of both sandy bottom areas and muddy bottom areas. The sediment distribution in the Ariake Sea is markedly non-homogeneous as depicted in Fig. 2 (Kamata, 1979). Silt and sand cover most of the sea bottom. Generally, the sand is located offshore and more fine-grained sediment is found along the shoreline. The silty sand and silty clay cover an area approximately corresponding to the average water depth <8 m as depicted in Figs. 1, 2.

In this study, two-dimensional depth-averaged finite difference numerical models are

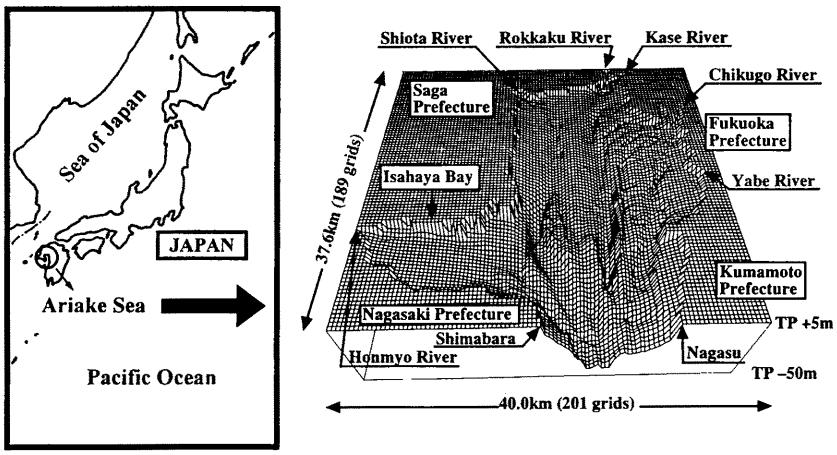

Fig. 1. Location and seabed topography of the Ariake Sea.

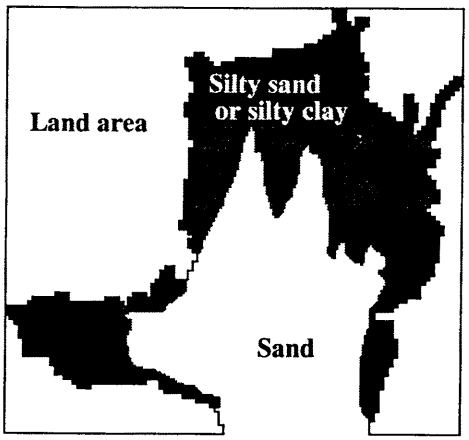

Fig. 2. Bottom sediment distribution in the Ariake Sea.

developed for predicting the tidal flow velocity and suspended sediment concentration (SS). In the suspended sediment transportation model, time–dependent resuspension, transportation and deposition are modeled as responses to the tidal flow by considering the presence of cohesive bottom sediment. The model results are compared with the in situ measurements of SS and tidal flow velocity at several stations in Isahaya Bay, which is located at the western part of the Ariake Sea as shown in Fig. 1, and with the concentration map of the Ariake Sea obtained from a Landsat Thematic Mapper (TM) image.

HYDRODYNAMIC MODEL

Governing equations

For calculating the tidal flow field, the assumption is made that the flow development is not influenced by the presence of suspended sediment. In situ measurements revealed that the maximum SS in the Ariake Sea was about 5,000 mg/*l* at the highest. This value results in a slight increase of 0.3% in density of seawater, which means that the above assumption is almost valid. Using the assumption and a right–hand coordinate system with $z=\eta$ at the sea surface and $z=-h$ at the seabed as shown in Fig. 3, the 2–dimensional depth–averaged shallow water equations for unsteady flow with hydrostatic pressure distribution can be written as follows:

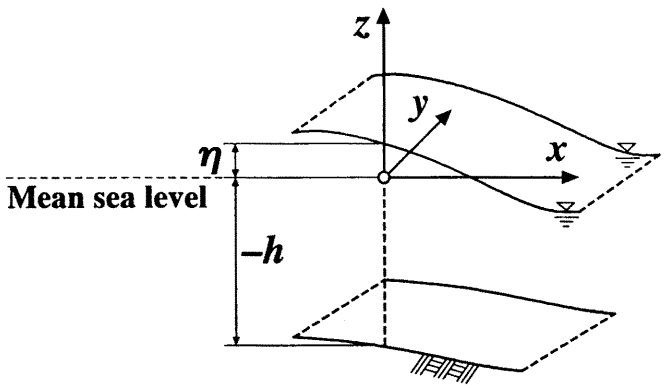

Fig. 3. Coordinate system used in the mathematical modeling.

$$\frac{\partial M}{\partial t}+\frac{M}{h+\eta}\frac{\partial M}{\partial x}+\frac{N}{h+\eta}\frac{\partial M}{\partial y}=\Omega N-g(h+\eta)\frac{\partial M}{\partial x}+\nu_h\left(\frac{\partial^2 M}{\partial x^2}+\frac{\partial^2 M}{\partial y^2}\right)-\frac{\tau_{b,x}}{\rho}+\frac{\tau_{s,x}}{\rho_{air}}, \quad (1)$$

$$\frac{\partial N}{\partial t}+\frac{M}{h+\eta}\frac{\partial N}{\partial x}+\frac{N}{h+\eta}\frac{\partial N}{\partial y}=-\Omega M-g(h+\eta)\frac{\partial \eta}{\partial y}+\nu_h\left(\frac{\partial^2 N}{\partial x^2}+\frac{\partial^2 N}{\partial y^2}\right)-\frac{\tau_{b,y}}{\rho}+\frac{\tau_{s,y}}{\rho_{air}}, \quad (2)$$

$$\frac{\partial \eta}{\partial t}+\frac{\partial M}{\partial x}+\frac{\partial N}{\partial y}=0, \quad (3)$$

where M, N are the flow rates over the depth in x– and y– directions. Using depth–averaged flow velocities in x– and y–directions, U and V, M and N are expressed as $(h+\eta)U$ and $(h+\eta)V$ respectively. The symbols ρ and ρ_{air} are used for the density of seawater and air; Ω is the Coriolis parameter; ν_h is the depth–averaged kinematic viscosity in the horizontal direction; g is the acceleration due to gravity and t is the time. The symbols $\tau_{b,x}$ and $\tau_{b,y}$ are the bottom shear stresses in x– and y–directions, $\tau_{s,x}$ and $\tau_{s,y}$ are the wind shear stresses on the sea surface in x– and y–directions respectively.

The bottom shear stress vector $\tau_b=(\tau_{b,x}, \tau_{b,y})^T$ was given with the use of Manning formula, the flow rate vector $\boldsymbol{B}=(M, N)^T$ and the Manning's coefficient of roughness n:

$$\boldsymbol{\tau}_b=\frac{\rho n^2 g \boldsymbol{B}|\boldsymbol{B}|}{(h+\eta)^{7/3}}, \tag{4}$$

where $|\mathbf{B}|$ denotes a norm of a vector $\boldsymbol{B}$. Equation (4) indicates that the bottom shear stress has the same direction as the depth–averaged velocity and depends quadratically on its magnitude.

Boundary conditions

The boundary condition along the open boundary line, which is the Shimabara–Nagasu line in Fig. 1, was given by the tidal levels calculated at Shimabara and Nagasu. The harmonic constants are obtained at Shimabara and Nagasu tidal stations located at both ends of the open boundary line. The tidal levels at any point on the open boundary line were given by linear interpolation of the tidal levels at both ends calculated by using the harmonic constants of seven component tides. In the following, the computational results are compared with the in situ measurements of SS and tidal flow velocity, which were

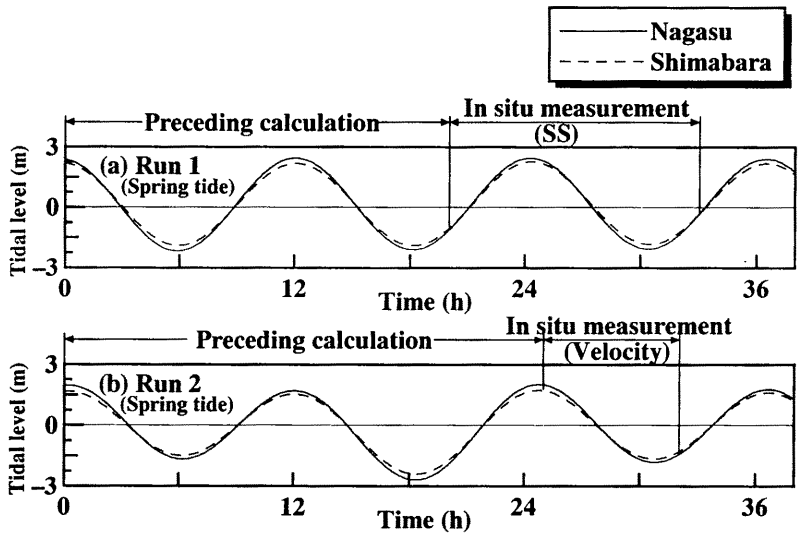

Fig. 4. Tidal levels at Shimabara and Nagasu calculated for (a) Run 1 and (b) Run 2.

Table 1. Date and time for the numerical simulations of the in situ measurements.

No.	Calculation	In situ measurement
Run 1	Sep. 12. 10:00(0)–14. 0:00(38), 1988	Sep. 13. 6:00(20)–19:00(33), 1988 (SS)
Run 2	Jan. 23. 10:00(0)–25. 0:00(38), 1989	Jan. 24. 11:00(25)–18:00(32), 1989 (Tidal flow velocity)

*( ): The cumulative time corresponding to the horizontal axis in Fig. 4.

executed at several stations in Isahaya Bay in 1988 and 1989 as depicted in Table 1. Figure 4 shows the tidal levels at Shimabara and Nagasu calculated for the calculation periods in Table 1.

In the Ariake Sea, parts of the sea area dry up at low water levels and the vast tidal flat appears due to the huge tidal range and the extremely gentle seabed slope. The moving land boundary was therefore adopted by using the threshold water depth $h_{min} \equiv (h+\eta)_{min}$ to determine the land boundary line (Kato *et al.*, 1988). This is because Eqs. (1), (2) have a singular character when $(h+\eta)=0$. Along the land boundary, the normal flow velocity to the boundary line was set to be zero, which means the free–slip condition (Kato *et al.*, 1988). River inflows were also considered for the six relatively large rivers that flow into the Ariake Sea as shown in Fig. 1.

Numerical scheme and parameters

The shallow water equations (1), (2), (3) were spatially discretized by rectangular staggered grids with grid sizes $\Delta x=\Delta y=200$ m, which results in 201×189 grids covering the study area as shown in Fig. 1. In this figure, the seabed topography was depicted in every two computational grids. The total number of the grids in the sea area is 18,518. The leap–frog scheme was adopted as time integration with a time step $\Delta t=5$s and the method of characteristics in one spatial dimension was incorporated into the calculation along the open boundary line.

As depicted in Fig. 4, the calculations started at the tidal condition of high water. The initial conditions were therefore determined as $(h+\eta)$=constant and $M=N=0$ on all grids in the sea area. The parameters used in the calculation of the shallow water equations are as follows: the Manning's coefficient of roughness $n=0.025\,\mathrm{m}^{-1/3}\mathrm{s}$; the threshold water depth $h_{min}=0.08$ m; the Coriolis parameter $\Omega=7.92\times10^{-5}\mathrm{s}^{-1}$; the depth–averaged kinematic viscosity $\nu_h=0$; the wind shear stresses on the sea surface $\tau_{s,x}=\tau_{s,y}=0$; the acceleration due to gravity $g=9.8\,\mathrm{m/s}^2$.

SUSPENDED SEDIMENT TRANSPORTATION MODEL

Governing equations

Using the flow rates M and N calculated from the shallow water equations (1), (2), (3), the 2–dimensional depth–averaged convective–dispersion equation for SS can be written as:

$$\frac{\partial\{C(h+\eta)\}}{\partial t}+\frac{\partial(CM)}{\partial x}+\frac{\partial(CN)}{\partial y}=\frac{\partial}{\partial x}\left\{(h+\eta)K_x\frac{\partial C}{\partial x}\right\}+\frac{\partial}{\partial y}\left\{(h+\eta)K_y\frac{\partial C}{\partial y}\right\}+\mathrm{P-S}, \quad (5)$$

where C is the depth-averaged SS, K_x and K_y are the convective-dispersion coefficients in x- and y-directions, P and S are the vertical flux of sediment resuspension and suspended sediment deposition, respectively.

Sediment resuspension

In the Ariake Sea, the sand is located offshore and the silty sand and silty clay are found along the shoreline as already depicted in Fig. 2. Most of the suspended sediment in coastal waters is constituted by fine-grained particles. In numerically predicting SS in the Ariake Sea, therefore, it is very important to estimate the critical shear stress and pick-up rate of fine-grained and cohesive sediment such as the silty sand and silty clay.

In the case of the non-cohesive sediment such as sand, the principal factors controlling erosion are the weight and size of the particles, while the resistance of cohesive sediment to erosion is prescribed by the electrochemical bond between individual particles. This is because the individual particles in cohesive sediment are much smaller and the weight of particles is normally an insignificant factor compared to the electrochemical forces. The threshold of erosion for non-cohesive sediment is characterized by a definite value of the well-known Shields' entrainment function. In cohesive sediment, however, this value would be increased by cohesion. In addition to this, Task Committee (1968) of ASCE summarized the research works on erosion and transportation of cohesive sediment in which there is no functional relationship between cohesion and a grain size. For the reasons stated above, the sediment resuspension was modeled on the results of both the laboratory experiment using the cohesive bottom mud sampled at the Ariake Sea (Umita *et al.*, 1988; Hiramatsu *et al.*, 1991; Kondo *et al.*, 1993) and the in situ measurements in Isahaya Bay (Kondo *et al.*, 1996).

The critical shear stress τ_{ce}=0.3 Pa obtained by Kondo *et al.* (1993, 1996) was used for judging the start of sediment resuspension. The pick-up rate E_r was estimated through the equation proposed by Umita *et al.* (1988):

$$E_r=\alpha\left(\frac{|\tau_b|}{\tau_{ce}}-1\right)^b, \quad |\tau_b|>\tau_{ce}, \quad (6)$$

where α and b are the parameters that should be determined by the experiments. The authors' experiments (Hiramatsu *et al.*, 1991; Kondo *et al.*, 1993, 1996) and in situ measurements (Kondo *et al.*, 1996) revealed the following facts. The resuspension of cohesive bottom mud in the Ariake Sea where a semi-diurnal current plays a prominent role did not continue in spite of $|\tau_b|>\tau_{ce}$ because of the hardening of its surface. The resuspension stopped at the time t_d after the start of it. This fact was considered in calculating the vertical flux P in Eq. (5).

Deposition of suspended sediment

The mass-balance equation considering the vertical diffusive transport explicitly, such as a 3-dimensional model, can automatically estimate the vertical mass flux from the quantitative balance between the vertical diffusion and deposition terms. On the other

hand, the depth-averaged model does not consider this balance, and the critical shear stress τ_{cd} of deposition should be given for judging the generation of deposition when $|\tau_b| < \tau_{cd}$. The experimental results (Kondo *et al.*, 1993, 1996) suggested the value of τ_{cd} =0.025 Pa which was used in the numerical computation. When $|\tau_b| < \tau_{cd}$, the vertical flux of suspended sediment deposition D_p was given by:

$$D_p = \omega_0 C, \quad |\tau_b| < \tau_{cd}, \tag{7}$$

where ω_0 is the particle settling velocity calculated by the Stokes' equation with the median diameter of suspended sediment in the Ariake Sea.

Computational procedure of time-dependent sediment resuspension and deposition

Figure 5 shows the computational procedure of time-dependent sediment resuspension and deposition used in the numerical computation. During about 12 hours from high water to low water or vice versa, the bottom shear stress rises from almost zero to a peak and then falls to almost zero. Using the bottom shear stress $|\tau_b|$ calculated by Eq. (4) at every computational grid, the vertical flux P and S of sediment resuspension and suspended sediment deposition in Eq. (5) were calculated at every computational grid as follows: 1) P=0, $S=D_p$; 2) P=0, S=0; 3) $P=E_r$, S=0; 4) P=0, S=0; 5) P=0, $S=D_p$. This procedure was applied to the sea areas covered by the silty sand and silty clay bottoms shown in Fig. 2. In sandy bottom areas, P is always zero and $S=D_p$ when $|\tau_b| < \tau_{cd}$.

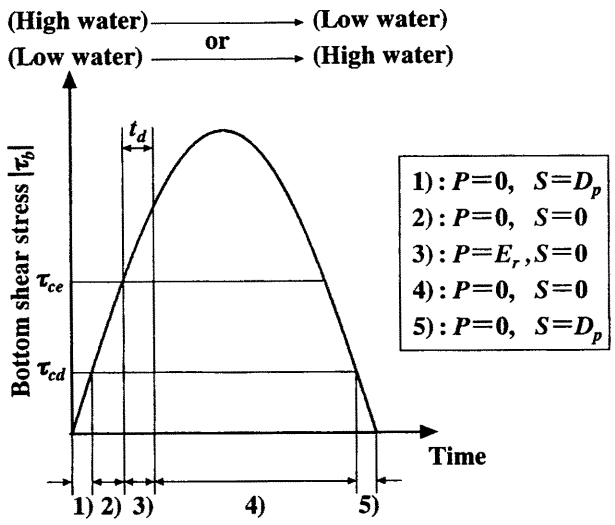

Fig. 5. Schematic diagram of the time-dependent resuspension and deposition.

Boundary conditions

The boundary condition along the open boundary line was given by the Dirichlet–type boundary condition, namely $C=C_b$ (=constant). The value of C_b was estimated through the in situ measurements of SS executed in Isahaya Bay as shown in Table 1. Along the land boundary, the normal flux of SS to the boundary line was set to be zero, which means the Neumann–type boundary condition. The increase of SS due to the sediment resuspension generated by waves was considered as the empirical manner, in which the value of SS is set to be 2,000 mg/l when a computational grid changes from in–land area to in–sea area. The suspended loads from rivers were also considered for the six relatively large rivers that flow into the study area as shown in Fig. 1. The suspended loads C_L were calculated through the equation:

$$C_L=\beta Q^{\gamma}, \tag{8}$$

where β and γ are the parameters that were estimated by in situ measurements for every river.

Numerical scheme and parameters

The convective–dispersion equation (5) was spatially discretized by rectangular unstaggered grids with grid sizes $\Delta x=\Delta y=200$ m, which correspond to the grids adopted in the discretization of the shallow water equations. The shifting particles method (Hiramatsu *et al.*, 1989), which is known as one of the operator splitting techniques, was used as time integration with a time step $\Delta t=20$ s. Considering the minimum SS observed in the in situ measurements, the initial conditions were determined as $C=4$ mg/l on all grids in the sea area. The convective–dispersion coefficients K_x and K_y were assumed to be 50 m^2/s through the experimental study of the tidal current and diffusive mixing in the head of the Ariake Sea (Tohara *et al.*, 1980).

The other parameters used in the calculation of the convective–dispersion equation are as follows: the parameters of pick–up rate $\alpha=6.2\times10^{-4}$ kg/(m^{2}s), $b=2.3$ and $t_d=0.5$ h; the particle settling velocity $\omega_0=10^{-4}$ m/s; the boundary condition along the open boundary line $C_b=4$ mg/l.

RESULTS AND DISCUSSION

Comparison with in situ measurements

The computational results of the model are compared with the in situ measurements of tidal flow velocity and SS in Isahaya Bay.

Figure 6 shows the comparison of the measured flow vectors at 10 measurement points in Isahaya Bay and the calculated flow vectors at the corresponding computational grids in Run 2. The measurement points were indicated on the map in Fig. 6 and the measurements were executed at the time interval of one hour. Good correspondence can be observed with regard to the magnitude and direction of tidal flow. Figures 7, 8 show examples of the calculated flow vectors in the study area. In these figures, the vectors were depicted in every three computational grids.

Figure 9 shows the comparison of the measured SS at 14 measurement points in

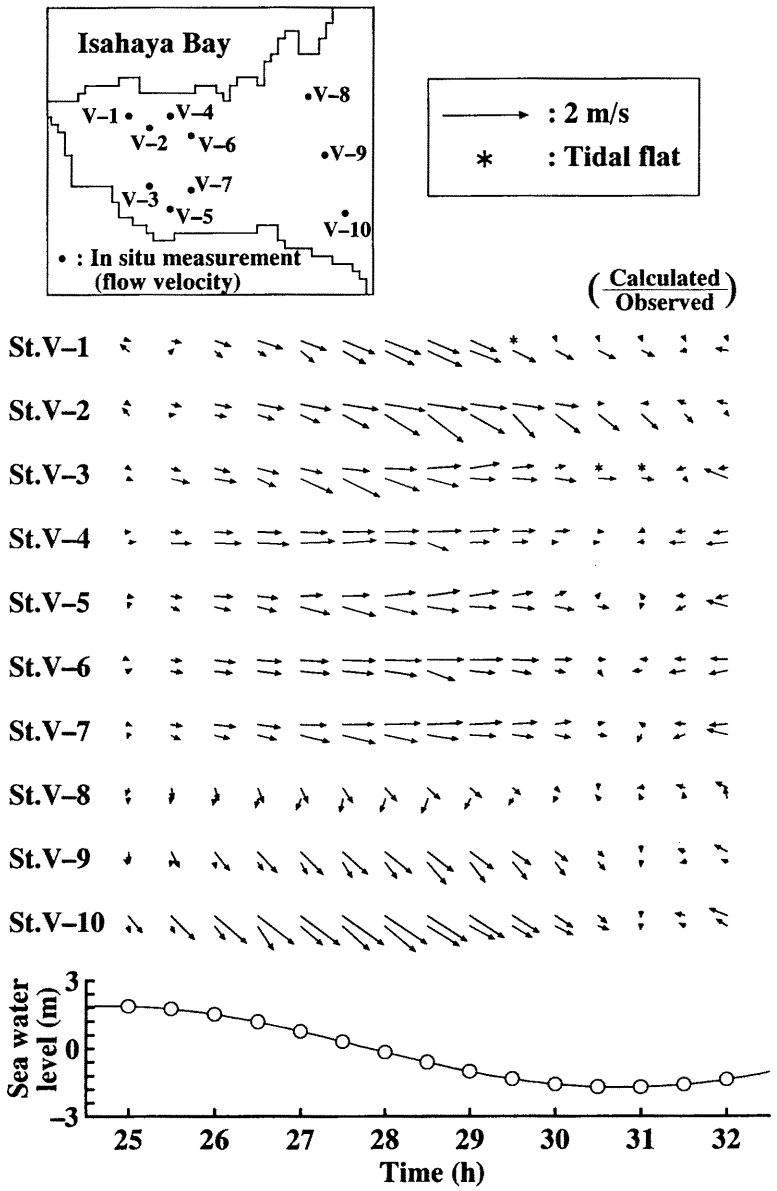

Fig. 6. Comparison of the in situ measurements of flow vectors in Isahaya Bay and the calculated flow vectors in Run 2.

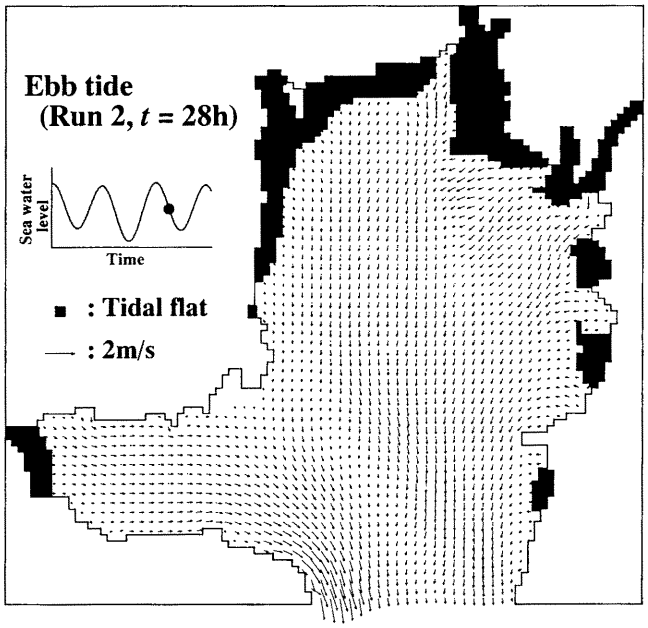

Fig. 7. Calculated flow vectors at ebb tide in Run 2.

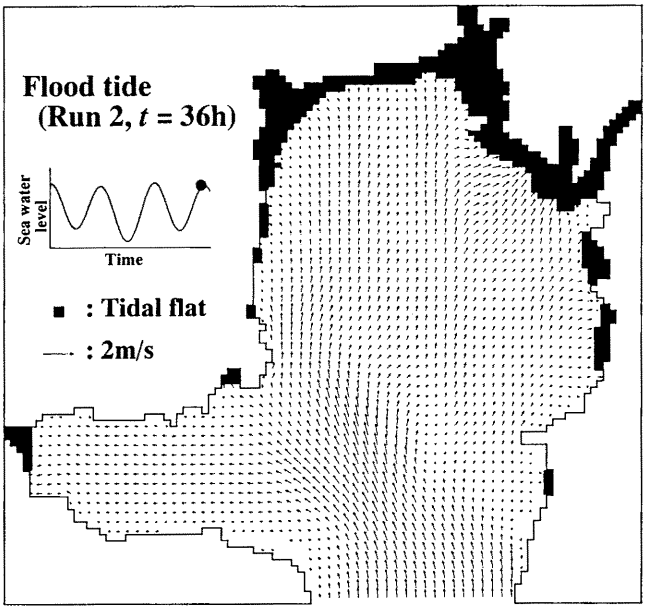

Fig. 8. Calculated flow vectors at flood tide in Run 2.

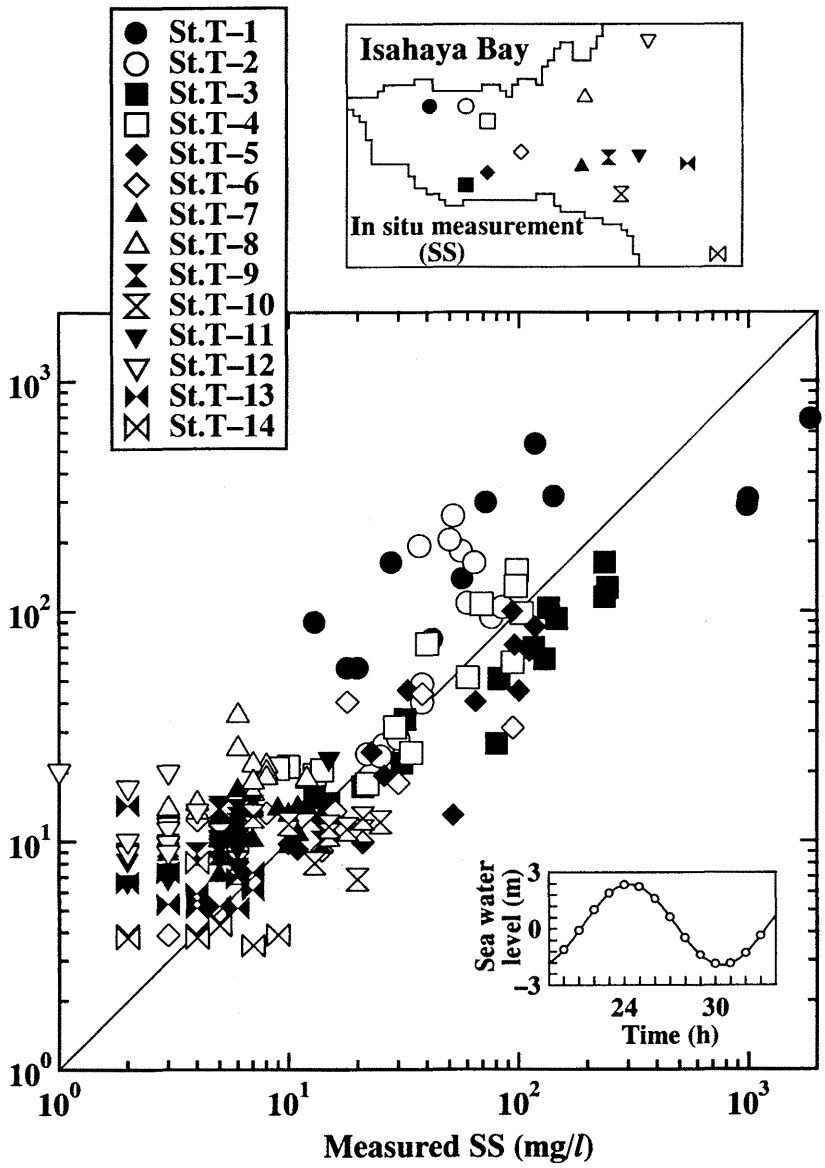

Fig. 9. Comparison of the in situ measurements of SS in Isahaya Bay and the calculated SS in Run 1.

Isahaya Bay and the calculated SS at the corresponding computational grids in Run 1. The measurement points were indicated on the map in Fig. 9. The values of SS at the vertical position of half depth were measured at the time interval of one hour. The agreement is generally good over the wide range of SS. Figure 10 shows an example of the concentration map of calculated SS in the study area.

Comparison with Landsat TM image

The concentration map of SS calculated from a Landsat TM image was also used to examine the spatial distribution of calculated SS. An image was recorded on September 13, 1988 when the in situ measurements of SS in Table 1 were executed. This image, however, could not be used for estimating the spatial distribution of SS due to the presence of clouds. The image recorded at 10:20 a.m. on April 15, 1988 along Path 113/Row 037 was selected because the tidal conditions on that day were approximately the same as those on September 13, 1988. The in situ measurements of SS on September 13, 1988 at the 14 points in Fig. 9 were used as sea-truth data. The concentration map of SS was calculated with the linear regression equation obtained from the averages of 6×6 pixel values of band-3 surrounding the 14 ground sampling sites and sea-truth data in Isahaya Bay. Band-3 had the maximum value of correlation coefficient among the seven band of Landsat TM image in the linear regression analysis. Figure 11 shows the concentration map of SS estimated through the procedure stated above. In this figure, the high concentration areas are found along the shoreline. Figure 10 is the calculated concentration map in Run 1 at the time of approximately the same tidal conditions as Fig. 11. There is again good agreement in the general pattern of spatial distribution of SS in Figs. 10, 11.

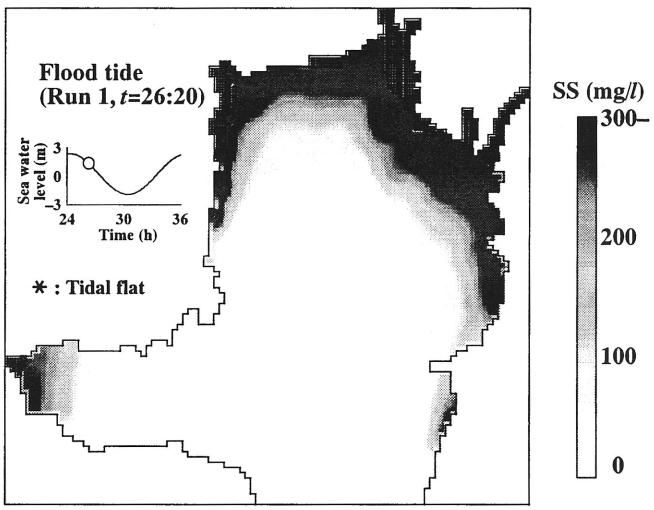

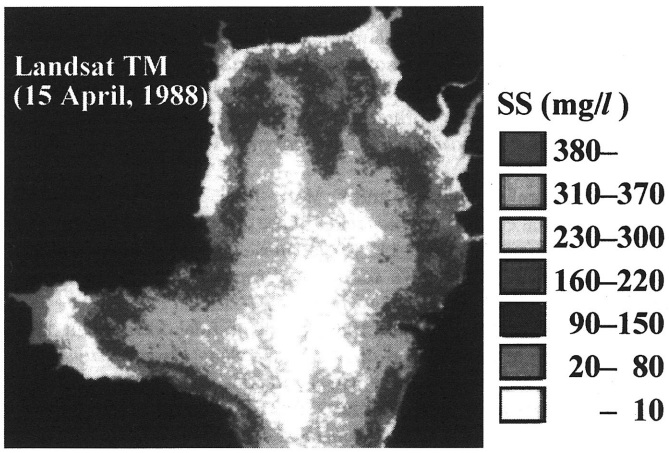

Fig. 11. Concentration map of the SS estimated from the Landsat TM image.

Conclusions

In this study, the 2-dimensional depth-averaged finite difference numerical models have been developed for predicting the tidal flow and SS in the Ariake Sea, Japan. In the suspended sediment transportation model, time-dependent sediment resuspension and deposition processes were modeled as responses to the tidal flow by considering the presence of the cohesive bottom sediment. The model results were compared with not only the in situ measurements of SS and tidal flow velocity at several stations in Isahaya Bay, but also with the concentration map of SS calculated from the Landsat TM image. It was concluded that the models with the time-dependent resuspension and deposition were capable of successfully and accurately reproducing the cohesive sediment transportation process in the Ariake Sea.

ACKNOWLEDGEMENTS

The authors wish to acknowledge Isahaya Bay Reclamation Project Office, the Kyushu Regional Agricultural Administration Office, Ministry of Agriculture, Forestry and Fisheries of Japan, for the acquisition of the in situ measurement data of the suspended sediment concentration and tidal flow velocity.

REFERENCES

Hiramatsu, K., Y. Tohara, S. Shikasho and K. Mori 1989 Numerical solutions of convective-dispersion equation for shallow sea by shifting particles and method of characteristics, *Scientific Bulletin of the Faculty of Agriculture, Kyushu University*, **44**(1·2): 39–46 (in Japanese with English summary)

Hiramatsu, K., Y. Tohara, S. Shikasho, K. Mori and A. Watanabe 1991 Experimental study on erosional process of cohesive bottom sediment by an annular flume, *Transaction of the Japanese Society of Irrigation, Drainage and Reclamation Engineering*, **151**: 39–48 (in Japanese with English summary)

Kamata, Y. 1979 Geomorphology and geology of the Ariake Sea, *Bulletin on Coastal Oceanography*,

17(1): 72–83 (in Japanese)

Kato, O., Y. Tohara and K. Mori 1988 Tidal current analysis for the Ariake Sea, *Proceedings of the International Symposium on Shallow Sea and Low Land*: 33–39

Kondo, M., K. Hiramatsu, Y. Tohara, S. Shikasho and K. Mori 1993 Physical properties of cohesive sediment materials and characteristics of their erosion by flow, *Transaction of the Japanese Society of Irrigation, Drainage and Reclamation Engineering*, **163**: 79–86 (in Japanese with English summary)

Kondo, M., Y. Tohara, K. Hiramatsu, S. Shikasho and K. Mori 1996 Characteristics of erosion on cohesive sedimentary materials by tidal current, *Transaction of the Japanese Society of Irrigation, Drainage and Reclamation Engineering*, **182**: 109–115 (in Japanese with English summary)

Task Committee 1968 Erosion of cohesive sediment, *Proceedings of American Society of Civil Engineers*, **194**(HY4): 1017–1049

Tohara, Y., K. Watanabe, O. Kato and M. Seguchi 1989 Study on tidal current and diffusive mixing in the Ariake Sea–Circulative current in the head of the Ariake Sea–, *Proceedings of the 27th Japanese Conference on Coastal Engineering*: 483–486 (in Japanese)

Umita, T., T. Kusuda, T. Futawatari and Y. Awaya 1988 Study on erosional process of soft mud, *Proceedings of the Japan Society of Civil Engineers*, **393**(II-9): 33–42 (in Japanese with English summary)